

Qualatative Analysis of Symmetric Modes of a Vibrating Drumhead

by

Matt Brozak

University of Central Arkansas
Conway, Arkansas 72032
Fall 2008

Abstract

The physical phenomenon of a vibrating drumhead can be accurately modeled by use of the two-dimensional wave equation. Solving this model makes it possible to predict the natural frequencies at which the fundamental mode and subsequent modes of vibration appear. Using a drum, driven by a subwoofer, amplifier, and signal generator the modes of vibration were successfully reproduced and were found to match the predicted modes of vibration.

1 Introduction

Drums have been essential to human interaction and communication since the beginning of civilization. As with any physical phenomenon, physicists have strove to understand and predict its behavior. Modeling and solving this problem is daunting at first, considering that two coordinates are needed to locate any point on the surface and another is necessary to determine displacement. To accomplish this feat, one can visualize a small element of the total surface as according to figure 1.

Specific assumptions are made to obtain a practical mathematical model. First, the membrane is assumed to be thin, to ensure an equation that only exists in two dimensions. Second, the membrane is assumed to be perfectly elastic ensuring that the model doesn't become overcomplicated with damping terms. Last, the membrane is to undertake only small displacements. Letting ρ_s be the surface density of the membrane [kg per m^2] and τ is the tension per unit area [N per m^2]. The derivation starts with Newton's Second law; The force acting on any one part of the surface is the sum of the net transverse forces acting along the x and z axes;

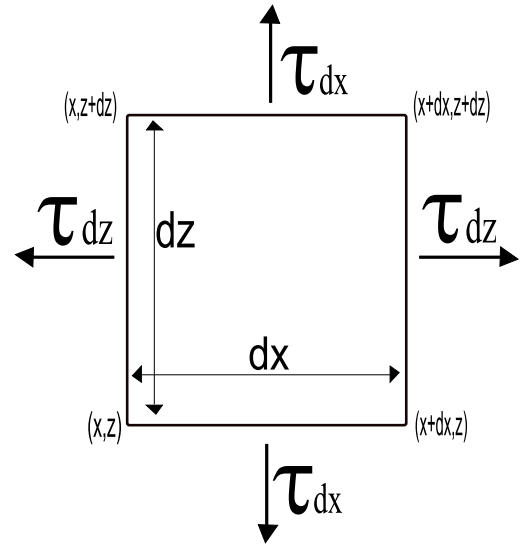


Figure 1: Segment of vibrating membrane.

$$\Sigma F_x = ma_x \tag{1}$$

and

$$\Sigma F_z = ma_z \tag{2}$$

From Figure 1, the net forces acting on the element are due to tensions in the x and z axis, respectively

$$\tau dz \left[\left(\frac{\partial u}{\partial x} \right)_{x+dx} - \left(\frac{\partial u}{\partial x} \right)_x \right] = \tau \frac{\partial^2 u}{\partial x^2} dx dz \quad (3)$$

and

$$\tau dx \left[\left(\frac{\partial u}{\partial z} \right)_{z+dz} - \left(\frac{\partial u}{\partial z} \right)_z \right] = \tau \frac{\partial^2 u}{\partial z^2} dx dz \quad (4)$$

The argument for the forces acting on the element are analagous to the argument for transverse waves acting on a string. u is the displacement away from equilibrium, and has the same physical characteristics as y from Appendix B. Summing the terms in accordance with Eq. 1 and 2 yields,

$$\tau \left(\frac{\partial^2 u}{\partial x^2} + \frac{\partial^2 u}{\partial z^2} \right) dx dz = \rho_s dx dz \frac{\partial^2 u}{\partial t^2} \quad \text{for } (x,z) \in \Omega \quad (5)$$

Where u is a function of x , z , and t , and Ω is the boundary of interest. A slight rearrangement of this relation leads to;

$$\frac{\partial^2 u}{\partial t^2} = c^2 \left(\frac{\partial^2 u}{\partial x^2} + \frac{\partial^2 u}{\partial z^2} \right) \quad \text{for } (x,z) \in \Omega \quad (6)$$

where c is the speed of the disturbance in the membrane;

$$c = \sqrt{\tau/\rho_s} \quad (7)$$

Just as the mathematical model is generalized from one-dimensional ideals, it will follow that the physical behavior of the two-dimensional model will assume similar properties. Previous study of the property of waves reveals that boundary conditions restrict frequencies of vibration to a discrete set. Similar behavior is expected from

vibrating membranes, only the boundary conditions will now include the type of support and also the shape of the perimeter of the membrane.[1] While a solution can be found using the traditional cartesian coordinate system, the solution would be sloppy and almost interminable. By choosing polar coordinates the solution will be greatly simplified. The governing equation now becomes:

$$\frac{\partial^2 u}{\partial t^2} = c^2 \left(\frac{\partial^2 u}{\partial r^2} + \frac{1}{r} \frac{\partial u}{\partial r} + \frac{1}{r^2} \frac{\partial^2 u}{\partial \theta^2} \right) \quad \text{for } 0 \leq r < a, 0 \leq \theta \leq 2\pi \quad (8)$$

Where a is the radius of the drum and θ compliments the radial position. To make this more symbolically simple this equation can be written as

$$U_{tt} = c^2 \left(U_{rr} + \frac{1}{r} U_r + \frac{1}{r^2} U_{\theta\theta} \right) \quad (9)$$

where $U = U(r, \theta, t)$ and $U_{tt} = \frac{\partial^2 u}{\partial t^2}$. Implementing the method of separation of variables leads to,

$$U_r = R'(r)\Theta(\theta)e^{i\omega t} \quad (10)$$

$$U_{rr} = R''(r)\Theta(\theta)e^{i\omega t} \quad (11)$$

$$U_{tt} = -\omega^2 R(r)\Theta(\theta)e^{i\omega t} \quad (12)$$

$$U_{\theta\theta} = R(r)\Theta''(\theta)e^{i\omega t} \quad (13)$$

Where $R' = \frac{dR}{dr}$. It is important to note that in choosing $e^{i\omega t}$ as the temporal component, that only the real part of this is used in the final solution. Substituting these values into Eq. 6 and multiplying by $\frac{r^2}{\Theta(\theta)R(r)}$, yields

$$-\omega^2 r^2 = c^2 \left(r^2 \frac{R''}{R} + r \frac{R'}{R} + \frac{\Theta''}{\Theta} \right) \quad (14)$$

Letting $k = \frac{\omega}{c}$ and grouping all like terms yields

$$r^2 \frac{R''}{R} + r \frac{R'}{R} + k^2 r^2 = -\frac{\Theta''}{\Theta} \quad (15)$$

To solve this problem a simultaneous solution must be determined, the only non-trivial solution occurs when this relation is set equal to $-m^2$. Rewriting the equation and relating it to the constant leads to

$$-\frac{\Theta''}{\Theta} = \frac{r^2}{R} \left(R'' + \frac{1}{r} R' \right) + k^2 r^2 = -m^2 \quad (16)$$

Solving the left side of the relation yields a harmonic solution in the following form

$$\Theta(\theta) = \cos(m\theta + \eta) \quad (17)$$

The η term is the initial phase angle and takes values of $(2\pi, 4\pi, \dots)$, according to the geometry of the drumhead. Also, because we require u to be a single valued function of position then $u(r, \theta, t)$ must equal $u(r, \theta + 2\pi, t)$. This requires that m to take integer values of $m = (0, 1, 2, \dots)$. [1] Our relation now takes the form

$$R'' + \frac{1}{r} R' + \left(k^2 - \frac{m^2}{r^2} \right) R = 0 \quad (18)$$

This is known as Bessel's equation, this relation has the general solution

$$R(r) = AJ_m(kr) + BY_m(kr) \quad (19)$$

By definition J_m and Y_m correspond the Bessel's functions of the first and second kind respectively. Because our boundary conditions include $r = 0$ then B must be zero, and due to the restriction that there can be no motion at the outer boundary, $R(a) = 0$. Using these conditions Eq. 18 now leads to a discrete set of solutions

where

$$R(a) = J_m(ka) = 0 \quad (20)$$

$$k_{mn} = \frac{j_{mn}}{a} \quad (21)$$

where a is the radius of the membrane and $j = j^{\text{th}}$ root of the Bessel function.

We now have a general solution in the form of

$$U_{mn}(r, \theta, t) = J_m(k_{mn}r) \cos(m\theta + \eta)e^{i\omega t} \quad (22)$$

Also a relation for the frequency of the system is defined as

$$f = \frac{ck}{\text{wavelength}} = \frac{j_{mn}c}{2\pi a} \quad (23)$$

where $c = \sqrt{\tau/\rho_s}$ and a is the radius of the membrane.

Though the solution doesn't lend a very visually pleasing equation set it is better appreciated graphically. Figure 2 shows a snapshot of the solutions of the governing equation. One would notice the subscripts (m, n) appended on many of the terms. These correspond to the nodal lines and nodal circles, respectively, and are apparent in Figure 2. The shading refers to the observed transversal motion of the drum. Each oppositely colored section of the drum is exactly 180 degrees out of phase with its affiliated section.

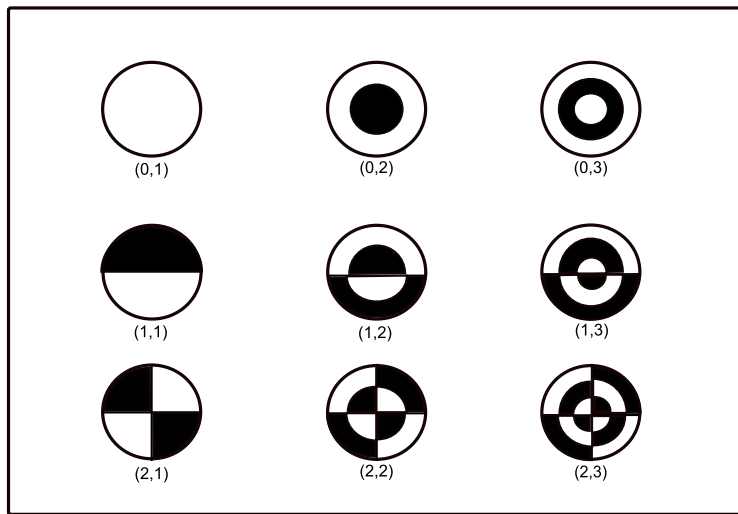


Figure 2: Modes of a circular membrane

2 Materials & Methods

To create uniform and constant oscillation of the drum, the apparatus incorporated a Pioneer A301R50-51F subwoofer driven by an Audio Source Amp1/A amplifier and an Agilent 33220A Wave Generator. For repeatability purposes the wiring diagram includes an ammeter and voltmeter. The current output is a direct

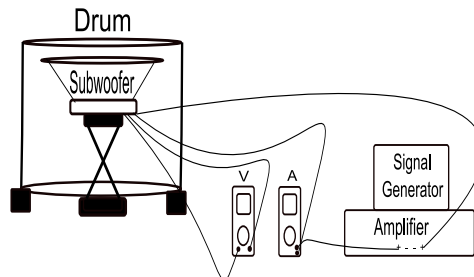


Figure 3: Setup for acoustically driven oscillation.

correlation to the power output from the amplifier. Because of the 8Ω rating on the subwoofer the current was not allowed to exceed $2.5A_{AC}$.

Since we are dealing with the vibrations of a symmetric surface, it is necessary to ensure as uniform a tension as possible. Modern day drums are kept “in tune” by adjusting the set screws around the top of the drum. The musician adjusts the tension by sound alone. Unfortunately this is not adequate for scientific experiment.

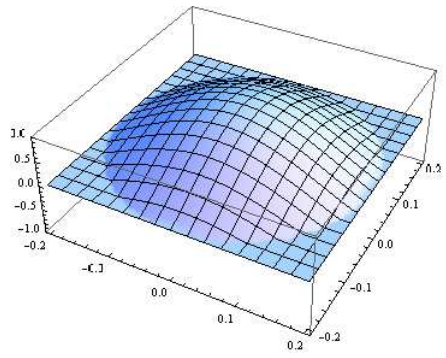
The drum was set so that there was an equal amount of threads showing from the bolt head on all clamps. After ensuring a roughly uniform tension, the apparatus was set so that there existed a 2 cm gap between the bottom of the drum and the top edge of the subwoofer. This was easily accomplished with a small lab jack. After a symmetric setup was assured the apparatus was powered up and allowed to warm up for fifteen minutes. This doesn't mean that one must simply turn on the power switches, but that a $0.5A_{AC}$ current is allowed to run through the circuit to also warm up the speaker. After a sufficient warm up period we must then visualize the vibrations. This is much harder than it seems. Depending on the color of the drum in use, in this case white, one can use a colored craft sand. The theory being that the sand will settle on the saddle points and be disturbed away from the oscillating sections of the surface. For this run of experiments a black craft sand (grain size $\frac{1}{16}mm - \frac{1}{8}mm$) was utilized.

There are two methods to determine the natural frequencies of vibration. One is to sweep through the available frequencies and wait for the sand to settle in symmetric patterns. While this is a viable method, one can also take advantage of previous work on this problem, present in almost any acoustics or advanced mathematics book. This knowledge leads to the mathematical property of vibrating membranes known as Bessel Functions. The fundamental mode will be the lowest frequency of vibration, once this mode is determined a quick calculation will give you an approximate value of the rest of the important modes of vibration, see Appendix A.

Recording the results can be done with any digital camera. Comparing these pictures or videos with Figure 2 makes it possible to draw a conclusion on the accuracy of the method.

3 Results

Results for the experiment were recorded by use of a digital camera. These pictures were then compared to the theoretical results compiled by a Mathematica program available in Appendix C and Figure 2. The results are on the next page:

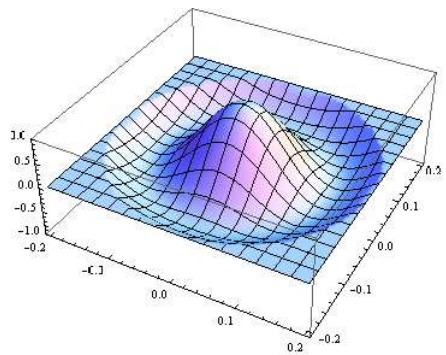


(a) Theoretical Mode



(b) Experimental Mode

Figure 4: Mode (0,1)

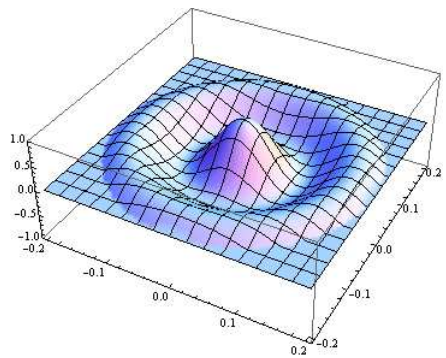


(a) Theoretical Mode



(b) Experimental Mode

Figure 5: Mode (0,2)

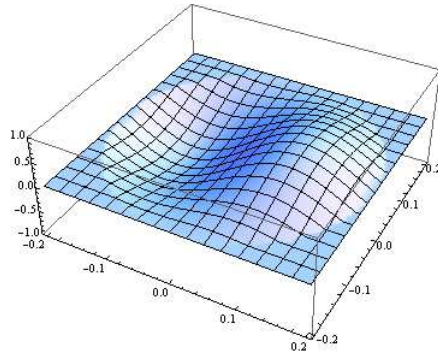


(a) Theoretical Mode



(b) Experimental Mode

Figure 6: Mode (0,3)

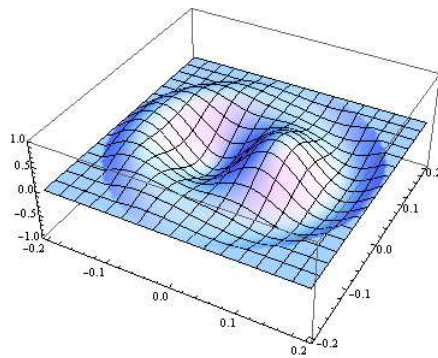


(a) Theoretical Mode



(b) Experimental Mode

Figure 7: Mode (1,1)

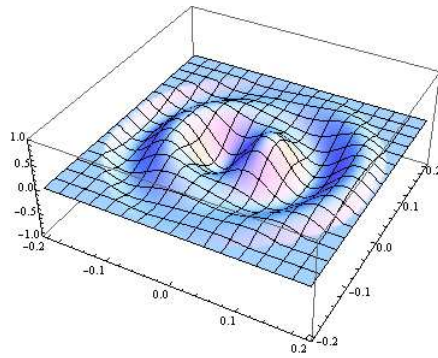


(a) Theoretical Mode



(b) Experimental Mode

Figure 8: Mode (1,2)

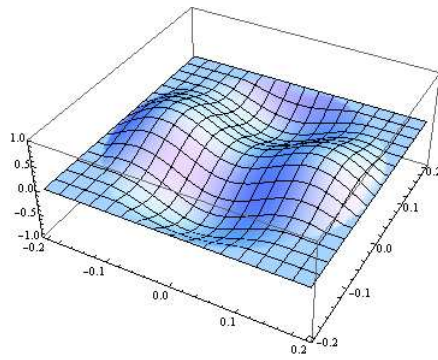


(a) Theoretical Mode



(b) Experimental Mode

Figure 9: Mode (1,3)

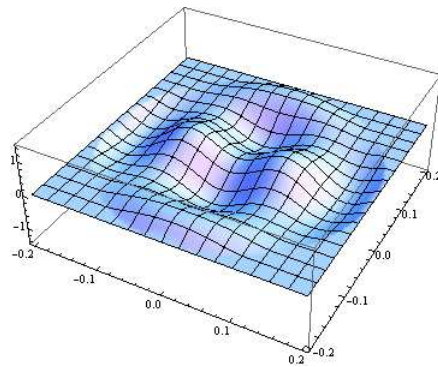


(a) Theoretical Mode



(b) Experimental Mode

Figure 10: Mode (2,1)

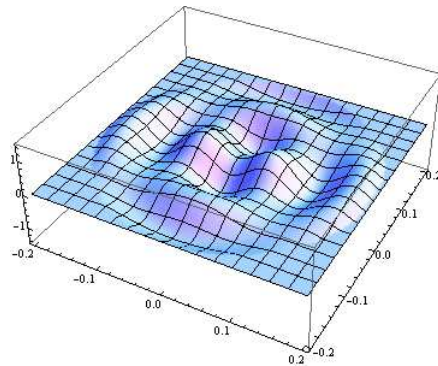


(a) Theoretical Mode



(b) Experimental Mode

Figure 11: Mode (2,2)



(a) Theoretical Mode



(b) Experimental Mode

Figure 12: Mode (2,3)

The following table is a listing of the corresponding frequencies compared between the theoretical and the observed. One will notice that the pictures above have modes that are not completely symmetric. Also there is a variance in the calculated and observed frequencies. The calculated frequencies are derived from the properties of Bessel's functions and circular boundary conditions, see Appendix A.

	Predicted Frequency (Hz)	Observed Frequency (Hz)	% Error
f_{01}	164.2	111.4	32.16
f_{02}	376.8	415	10.14
f_{03}	590.7	665	12.58
f_{11}	261.5	261.5	0
f_{12}	497.9	490.5	1.49
f_{13}	694.5	647.3	6.80
f_{21}	350.5	364	3.85
f_{22}	574.7	535	6.9
f_{23}	793.4	701	11.65

Table 1: Data table with comparison of predicted and observed frequencies.

4 Discussion

An astute observer would look at the percent error of the data and immediately raise questions. Not only is there a trend, but it seems that this trend picks an arbitrary absolute answer in f_{11} , and deviates away in both directions. This is due to the choice to not disassemble the drum, thus risking the integrity of the instrument. From Appendix A one can see that all subsequent modes of the drum are determined by a constant related to the Bessel's function and the fundamental mode f_{01} . This fundamental mode is a function of both tension and density of the drumhead. By not disassembling the drum and taking qualitative measurements of both of these physical constants an assumption must be made. Using Figure 2, one can see that f_{11} is the best candidate. This mode has a very distinct saddle point that runs across the diameter of the drum. The aforementioned assumption was made to discover the frequency for f_{01} and Table 2 was used to calculate values for the expected frequencies.

As one can see from the results section, everything does not follow theory. While the arbitrary coordinates that Mathematica supplies may confuse an observer, it is mainly a semantic problem. What does become a problem stems directly from the assumptions made at the beginning of the derivation of the theory. Assumption three states that the drumhead is *perfectly* elastic. This is obviously not true, and manifests itself in the sometimes odd patterns observed in Figure 12. Comparing the theoretical and experimental results, there are twice as many outside saddle points. Also only one of the two inner conical excitation points makes themselves evident. One can make the direct correlation between the relatively high frequency and the internal dampening that would occur, thus causing an increased % error. The unusually high error for f_{01} most likely manifests itself through the harmonics of the drum casing itself.[2] It was observed that during the frequency modulation to determine the fundamental mode; the drum struck its natural resonance frequency. This increased vibration would be

the most likely culprit for the unusually high % error.

Unfortunately, the human eye is not quick enough to catch these high frequency modes of vibration. This led to the use of sand to visualize a dynamic process. While this seemed to work fairly well, it did not perform to expectations when used with modes that have slightly ambiguous saddle points. This is especially the case in Figures 6 and 9. Objectively observing the theoretical mode from either of these figures shows saddle points that are nowhere near as stable as f_{11} .

5 Conclusion

This experiment proved itself to be a challenging exercise in mathematical derivation. The apparatus used, while simple in design, ultimately led to a deviation from the accepted behavior of the theoretical results. The vibrational *characteristics* of a drum can be modeled by generalizing the two-dimensional wave equation, while the qualitative results will vary. Many of the assumptions for this model hinge on an ideal world. As experiment almost always proves, the real world is never precisely predicted by mathematical theory. Though this theory does point the inquiring mind into the right direction, it cannot be used as an accurate method to totally predict the behavior of vibrating membranes. A more thorough approach, including manufacturing your own membrane from more trustworthy and measurable material, and physically ensuring uniform tension and density would most likely lead to better visualization of the nodal lines.

6 Appendix A

Appendix A contains information pertaining to the Bessel's function as well as previous modal information, where

$$f_{mn} = \frac{j_{mn}c}{2\pi a} \quad (24)$$

$f_{01} = 1.0f_{01}$	$f_{11} = 1.593f_{01}$	$f_{21} = 2.135f_{01}$
$f_{02} = 2.295f_{01}$	$f_{12} = 2.917f_{01}$	$f_{22} = 3.500f_{01}$
$f_{03} = 3.598f_{01}$	$f_{13} = 4.230f_{01}$	$f_{23} = 4.832f_{01}$

Table 2: Relative Theoretical Frequencies

7 Appendix B

To derive the equation of motion for a transverse wave on a string, one starts with the diagram below.

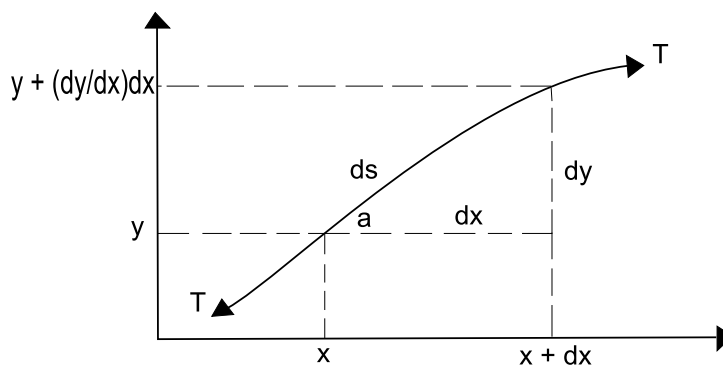


Figure 13: String Segment

The string is assumed to have uniform linear density and is stretched to a tension T . The figure represents an infinitesimal section of the string. Equilibrium is at x and has a length dx . y is the transverse displacement of the string from equilibrium, therefore

$$\partial f_y = (T \sin(a))_{x+dx} - (T \sin(a))_x \quad (25)$$

where a is the angle between the x axis and the tangent of the element of string, and two terms are the value of the tension at position $x + dx$ and x , respectively. The Taylor series expansion of this type of function is

$$f(x + dx) = f(x) + \left(\frac{\partial f}{\partial x}\right)_x dx + \frac{1}{2} \left(\frac{\partial^2 f}{\partial x^2}\right)_x dx^2 + \dots \quad (26)$$

Applying this concept yields

$$\partial f_y = [(T \sin(a))_x + \frac{\partial(T \sin(a))}{\partial x} dx + \dots] - (T \sin(a))_x = \frac{\partial(T \sin(a))}{\partial x} dx \quad (27)$$

This solution takes advantage of the fact that the first partial term of the Taylor series dominates all subsequent terms. If a is small then $\sin a$ can be replaced by $\frac{\partial y}{\partial x}$, in accordance with the small angle approximation which states $\sin a \approx \tan a$. The transverse force acting on the string now becomes

$$\partial f_y = \frac{\partial(T \frac{\partial y}{\partial x})}{\partial x} dx = T \frac{\partial^2 y}{\partial x^2} dx \quad (28)$$

Using Newton's second law and equating the sum of the forces to ma we now have

$$\Sigma F_y = ma_y \quad (29)$$

$$T \frac{\partial^2 y}{\partial x^2} dx = \rho_L dx \frac{\partial^2 y}{\partial t^2} \quad (30)$$

where $\rho_L dx$ is the mass of the string and the second partial of y with respect to t

is the calculus equivalent of acceleration. Rewriting leaves the final form

$$\frac{\partial^2 y}{\partial x^2} = \frac{1}{c^2} \frac{\partial^2 y}{\partial t^2} \quad (31)$$

where,

$$c^2 = \frac{\tau}{\rho_L} \quad (32)$$

8 Appendix C

The following is the Mathematica code that will export a (.gif) movie into “My Documents”.

```
Plot[{BesselJ[0, x], BesselJ[1, x]}, {x, 0, 20}]
Clear[alpha], f, k, [lambda]]
[alpha][0, j_] :=
  w /. FindRoot[BesselJ[0, w] == 0, {w, (j - 1)*[pi], j*[pi]}]
[alpha][1, j_] :=
  w /. FindRoot[
    BesselJ[1, w] == 0, {w, [alpha][0, j], [alpha][0, j + 1]}]
[alpha][2, j_] :=
  w /. FindRoot[
    BesselJ[2, w] == 0, {w, [alpha][1, j], [alpha][0, j + 1]}]
[alpha][3, j_] :=
  w /. FindRoot[
    BesselJ[3, w] == 0, {w, [alpha][1, j], [alpha][2, j + 1]}]

[alpha][4, j_] :=
```

```

w /. FindRoot[
  BesselJ[4, w] == 0, {w, [alpha][1, j], [alpha][3, j + 1]}]
a = .2;
[sigma] = .05;
T = 100;
c = Sqrt[T/[sigma]];
k[m_, n_] := [alpha][m, n]/a;
[lambda][m_, n_] := c*k[m, n];
f[m_, n_] := [lambda][m, n]/(2 [pi])
f[0, 2]
List[Table[f[i, s], {i, 0, 3}, {s, 1, 3}]]
r[x_, y_] = Sqrt[x^2 + y^2];
[theta][x_, y_] = If[x > 0, ArcTan[y/x], ArcTan[y/x] + [\pi]];
u[i_, s_, x_, y_, t_] =
  If[Sqrt[x^2 + y^2] < a,
    BesselJ[i, k[i, s] r[x, y]] Cos[i*[theta][x, y]]
    Cos[[lambda][i, s]*t], 0];
Plot3D[u[0, 3, x, y, 0], {x, -.2, .2}, {y, -.2, .2},
  PlotPoints -> 30];
Export["Drum02.gif", {Table[
  Plot3D[u[0, 2, x, y, .0001*j], {x, -.2, .2}, {y, -.2, .2},
    PlotPoints -> 30, PlotRange -> {-1, 1}], {j, 0, 110}]}]

```

The last line of code can be adapted to any integer value for m, n . This example will export the $f_{0,2}$ mode, where 110 frames will be output and the step size is $.0001j$.

9 Works Cited

References

- [1] L.E. Kinsler, A.R. Frey, A.B. Coppens, and J.V. Sanders. *Fundamentals of Acoustics*, 3rd edition. John Wiley & Sons, New York, NY, 1982.
- [2] Rossing, Moore, and Wheeler. *The Science of Sound*, 3rd edition. Pearson Education Inc, San Francisco, CA, 2002.